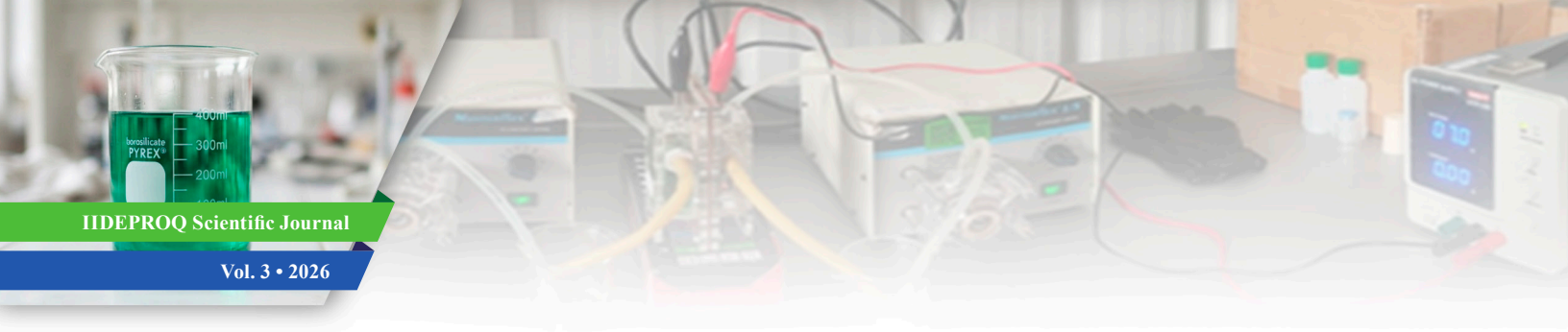


IIDEPROQ Scientific Journal
Vol. 3 • 2026

RECOVERY OF NICKEL AND COBALT FROM SPENT NI-MH BATTERIES BY ELECTROCHEMICAL PROCESS IN THE CITY OF LA PAZ

Jhosep Lendy Aliaga Luque[1], Boris Párraga Andrade[1,*]

ABSTRACT

Global demand for electronic devices is growing rapidly due to the need to keep pace with technological advancements. These devices rely on batteries with limited lifespans, resulting in significant quantities of electronic waste. The increasing generation of nickel-metal hydride (Ni-MH) battery waste in the city of La Paz poses an environmental problem due to the presence of potentially polluting metals, such as nickel and cobalt. Consequently, there is a need to develop sustainable recycling methods. This research involved recovering nickel and cobalt through a combination of leaching and electrodeposition. Used batteries were collected, discharged, dismantled, and ground. The resulting powders were then leached, purified to remove contaminants, and processed in a two-compartment electrochemical cell separated by an ion-exchange membrane (F-9010), using a platinum anode and a stainless steel cathode. The effects of temperature, voltage, and operating time were evaluated. An electrodeposit with nickel and cobalt concentrations exceeding 97 % was obtained. The optimal parameters identified were a temperature of 45 °C, a voltage of 8 V, and an operating time of 5 hours.

Keywords: Electronic waste, Electrowinning, Nickel, Cobalt.

1. INTRODUCTION

The rapid growth of the electronics industry and energy storage technologies has significantly increased the production and consumption of rechargeable batteries worldwide. In Bolivia, each person generates six kilograms of technological waste per year, totaling almost 80,000 tons annually (Bolrec, 2024). Among these, nickel-metal hydride (Ni-MH) batteries continue to be widely used in electronic devices, portable tools, energy backup systems, and hybrid vehicles due to their high storage capacity, operational safety, and long lifespan (Panasonic s.f.; Allied market research, 2023). However, once their life cycle is complete, these spent batteries become hazardous waste containing potentially toxic metals, such as nickel and cobalt, capable of contaminating soils, surface waters, and ecosystems when disposed of without adequate treatment. Several studies have pointed out that the improper disposal of electronic waste represents a growing environmental challenge, especially in developing countries where recycling systems are still limited (Hariprakash, 2009; Riswan et al.2024). Concurrently, the global demand for nickel and cobalt continues to rise due to their application in rechargeable batteries, special alloys, aerospace industries, and renewable energy technologies. According to international market reports, the sustained growth of these sectors is generating increasing pressure on primary mineral resources, the extraction of which involves high economic, energetic, and environmental costs (Mordor Intelligence, 2026; USGS, 2022).

[1] IIDEPROQ. Chemical Engineering. Faculty of Engineering. UMSA
***Corresponding author:** borisparraga@gmail.com

https://doi.org/10.53287/2026.9x2m4p1k

The importance of recovering these metals lies not only in mitigating the environmental impacts associated with electronic waste but also in the possibility of reincorporating them into productive cycles under the principles of the circular economy. In this context, hydrometallurgy and electrochemical processes have attracted growing interest due to their capacity to recover high-value metals with lower energy requirements and less secondary waste generation compared to conventional pyrometallurgical processes (Yu et al., 2018).

Addressing this issue has economic, technological, environmental, and scientific implications. From an economic perspective, the valorization of hazardous waste can contribute to reducing the dependence on raw materials from conventional mining. In the technological field, the study provides elements for the development and optimization of electrochemical processes applied to the recycling of electronic waste. Likewise, the implementation of sustainable management alternatives can reduce the environmental risks associated with the improper disposal of batteries. From a scientific standpoint, the research generates experimental information on the joint recovery of nickel and cobalt through electrodeposition and contributes to the knowledge related to the valorization of strategic metals.

Consequently, this research is framed within the principles of sustainability, the circular economy, and the efficient use of resources, evaluating a treatment alternative for spent Ni-MH batteries generated in the city of La Paz, with potential application in similar contexts.

Ni-MH batteries contain valuable metals: approximately 44% nickel, 5% cobalt, 2% zinc, and 9% light and rare earth metals (Shin et al., 2015). The elements present in the highest proportions are K, Ni, Co, and Zn. Nickel is found in both the cathode and the anode, whereas cobalt is primarily located in the anode.

There are few articles on hydrometallurgical and electrochemical processes for the recycling of Ni-MH batteries; leaching in each case is performed with acids such as H_2SO_4 at 90 °C for 4 h (Bertoul et al., 2012), 3N HCl at 90 °C for 3 hours (Rabah et al., 2008), 4M HCl at 95 °C for 3 hours (Tzanetakis et al. 2004), 5% v/v Acetic Acid (Zambrano et al., 2018), and in Lupi et al (2002), a comparison is made between HCl, H_2SO_4, and HNO_3, concluding that H_2SO_4 is the most suitable option for this process.

Because the leachate solution contains impurities (Mn, Al, Zn, Cu, rare earths) in its composition, it undergoes a purification step as indicated by (Tzanetakis et al. 2004), to remove rare earths, a 25% bis(2-ethylhexyl) phosphoric acid (D2EHPA) solvent in kerosene is used, separating into an organic phase and a raffinate (Hernandez et al. 2016), or, as indicated by Bertoul et al., (2012), by increasing the pH to 1.2 through the addition of 5 M sodium hydroxide, rare earths are removed as sulfates. Selective precipitation is one of the simplest and, therefore, most widely used methods, achieving efficiencies above 90% for metal recovery. The precipitation order of the metals is specific and depends on the value of the solubility product constant (pKs) (Pagani, 2021).

The solution obtained after rare earth recovery undergoes a second precipitation stage at pH 6 to remove Fe, Zn, and Mn, leaving Ni and Co in solution. The results demonstrated that Fe could be completely removed. As for Mn, only a poor removal efficiency of around 2.3% was achieved. For the complete precipitation of Mn, a pH of approximately 10 was required. Zn could be removed by approximately 24.0%. The precipitation of Ni usually begins at around pH 6.5, but in this case, probably due to a higher quantity of Ni compared to other metals, it was observed that at pH 6, about 0.5% of Ni co-precipitated. Regarding Co, about 2.2% was lost during precipitation (Bertoul et al., 2012).

Electrodeposition is carried out in an electrochemical cell with two compartments separated by an ion-exchange membrane. The process is based on the differences between the reduction potentials of the metals present, which favors their recovery with high purity. One of the advantages of this method is that it does not require external agents to recover the metals and can achieve yields close to 99% (Pagani, 2021).

Finally, considering the need to develop sustainable alternatives for the management of electronic waste and the utilization of strategic metals, the main objective of this research is to recover nickel and cobalt from spent nickel-metal hydride (Ni-MH) batteries through an electrochemical process based on acid leaching, solution purification, and electrodeposition. To achieve this purpose, the characterization of the active materials presents in the batteries, the evaluation of the leaching efficiency of the metals contained in the electrodes, and the determination of the most suitable operating conditions for electrodeposition were proposed.

Additionally, this study sought to analyze the influence of process variables such as temperature, applied voltage, and operating time on the recovery of nickel and cobalt, in order to establish optimal parameters that maximize the system's efficiency. Complementarily, it was proposed to evaluate the purity and composition of the obtained products to determine their reuse potential in industrial applications.

As an additional contribution, the research aims to demonstrate the technical and environmental viability of using electrochemical processes for the valorization of spent Ni-MH battery waste, promoting a recycling alternative that contributes to the circular economy and the reduction of dependence on primary sources of nickel and cobalt. In this context, the hypothesis posed is that optimizing the electrodeposition conditions allows for obtaining high-purity metal deposits and high recovery percentages, establishing it as an efficient solution for the treatment and utilization of this type of electronic waste.

2. MATERIALS AND METHODS

2.1. Materials

We used spent AA and AAA batteries, which were dismantled under a fume hood. A heating system with magnetic stirring was used for the leaching process.

We conducted the electrochemical tests using two peristaltic pumps, a direct current (DC) power supply, an electric heater, stainless steel electrodes as the cathode, and platinum as the anode, in addition to a Flemion-type ion-exchange membrane (F-9010).

The measurement instruments included an analytical balance, a digital thermometer, a pH meter, and a digital multimeter.

We monitored the process using atomic absorption spectrophotometry (AAS), X-ray diffraction (XRD), and X-ray fluorescence (XRF).

The X-ray diffraction (XRD) equipment is a PANalytical X'Pert-3 Powder model, operating with a Cu tube and generating X-ray radiation at 40 kV and 40 mA. We performed a scan between 3° and 60° under fully automated

conditions. We conducted this analysis on the collected and milled initial product for all heavy and light elements, yielding relative abundance estimation data, as shown in Table 2.

The X-ray fluorescence (XRF) equipment is a Rigaku GeigerFlex model, operating with a Cr tube at 50 kV and 30 mA. The recording process consists of two parts: an automatic run covering a range from 10° to 65° to determine the presence of heavy elements, and a manual run at specific ranges corresponding to light elements. We performed this analysis for heavy and light elements present in the initial sample, specifically, the cathodic and anodic powder from the batteries, yielding relative abundance estimation data.

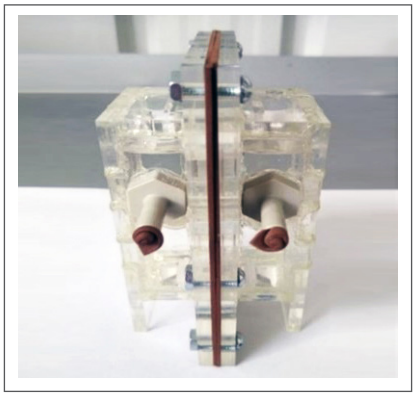
For atomic absorption spectroscopy (AAS) analysis, a Hitachi Model 180-30 instrument was used. The analyses were performed to determine nickel and cobalt concentrations in the recovered product, both in its solid form and after dissolution. The leachate solution was analyzed for nickel, cobalt, manganese, potassium, and zinc, while the battery powder was analyzed for nickel and cobalt.

2.1.1. Electrochemical Cell

We designed the electrochemical cell aiming to: reduce the compartment volume without impeding the solution flow (50 mL per compartment), utilize the maximum possible electrode surface area (15 cm^2), and minimize the distance between the electrodes as much as possible (2.5 cm). For the cell's construction, we used high-strength transparent acrylic and dielectric adhesive, as shown in 1.

The system operated continuously and hermetically, featuring polymeric gaskets designed to prevent liquid leaks.

Figure 1. Electrochemical Cell



Source: Prepared by the authors

2.1.2. Flemion 9010 Membrane

The membrane plays a fundamental role in electrolysis systems by separating the reaction compartments and controlling ion transport. Its use favors the separation of the cathodic and anodic reactions and reduces rapid pH variations, which can improve process efficiency (Moets et al., 2014).

Table 1 presents the normal and maximum operating values of the Flemion F-9010 membrane, within which it can operate without sustaining damage.

Table 1. Flemion F-9010 Membrane

Item	Normal	Max. Value	Unit
Current density	1<6	6 <7	kA/m^2
Voltage	0 a 6	<10	V
Temperature	60	80	°C

Source: Adapted from Rabah & Farghaly (2008)

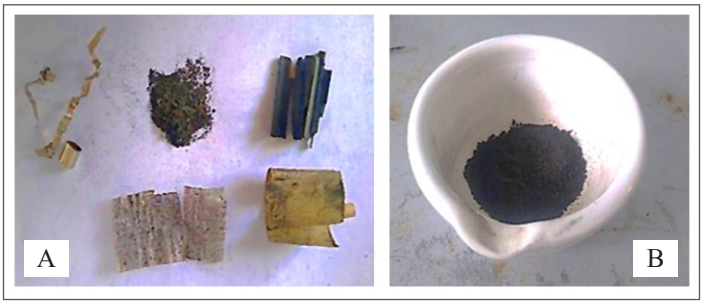
2.2. Methods

2.2.1. STAGE 1 Battery pretreatment

Before dismantling, the batteries were discharged in a 1% w/w NaCl solution to reduce the risks associated with residual energy. This procedure has been reported to achieve battery discharge without compromising the integrity of the casing. (Lu et al., 2013).

After discharging the batteries and separating their components, the cathodic and anodic materials were milled, as shown in Figure 2.

Figure 2. Battery pretreatment



Source: Prepared by the authors

Figure 2 shows: A) the metallic casing, the anodic powder, the cathodic powder, the support mesh for the anodic material, and the separator containing the battery electrolyte; and B) the anodic and cathodic powders after milling.

2.2.2. STAGE 2 Leaching and purification

After pretreatment, we subjected the cathodic and anodic materials to leaching to solubilize the metals present. We used a 2 M H_2SO_4 solution at 90 °C for 4 h, with constant stirring and a solid-to-liquid ratio of 1:30.

Figure 3. Left: the leaching system, and Right: the leachate



Source: Prepared by the authors

We separated the rare earths present in the leachate through selective precipitation. To achieve this, we adjusted the pH to 1.2 by adding sodium hydroxide. To purify the solution obtained after rare earth recovery, a second precipitation stage at pH 7 removes practically all the iron and over 70% of the total zinc (Bertoul et al., 2012).

2.2.3. STAGE 3 Electrodeposition of nickel and cobalt

This process utilizes two electrodes and relies on electrochemical oxidation and reduction reactions. The separation of the metals depends on the differences in their reduction potentials, enabling the recovery of high-purity products.

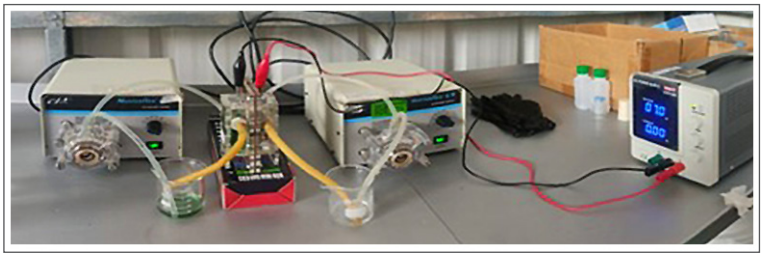
Studies on nickel recovery from nickel-metal hydride batteries establish the following reaction:

$$Ni(ac)^{2+} + 2H_2O(l) \rightarrow Ni(s) + 2H(ac)^{+} + O_2(g) + H_2(g)$$

As well as the electrowinning reaction for cobalt:

$$Co(ac)^{2+} + 2H_2O(l) \rightarrow Co(s) + 2H(ac)^{+} + O_2(g) + H_2(g)$$

Figure 4. Electrolysis System

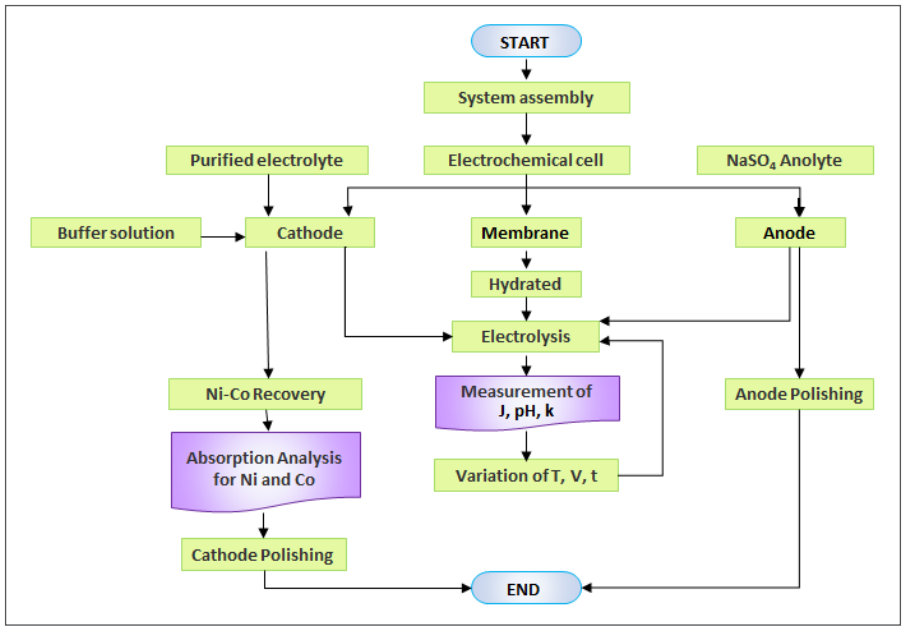


Source: Prepared by the authors

Figure 4 shows the system used for electrodeposition. The anode was platinum and the cathode was stainless steel; both had an active area of 15 cm². After electrodeposition, the deposit was collected for subsequent analysis.

Experiments were conducted at different temperatures, voltages, and operating times. For these tests, we kept the concentration of the purified electrolyte used as the catholyte constant (1,688 mg/L of cobalt and 9,625 mg/L of nickel), as well as the concentration of the Na_2SO_4 anolyte (1 M), reaching a current density of 250 A/m². The continuous process is shown in Figure 5.

Figure 5. Schematic of the process carried out for the objective of the project



Source: Prepared by the authors

3. RESULTS AND DISCUSSION

3.1 Battery dismantling

We performed an X-ray fluorescence (XRF) analysis to identify the elements present in the cathodic and anodic powders obtained from the dismantled batteries and used in the study.

Table 2. Battery powder components

Components	Elements
Major	K, Ni, Co, Zn
Minor	La, Nb, Mn
Trace	Na, Fe, Y, Pb

Source: XRD Laboratory Report (IGEMA)

We also conducted an atomic absorption analysis for nickel and cobalt; the results are shown in Table 3. The analyses indicate that the initial battery powders contain 6.5% cobalt and 50% nickel.

Table 3. Nickel and cobalt concentration in battery powder

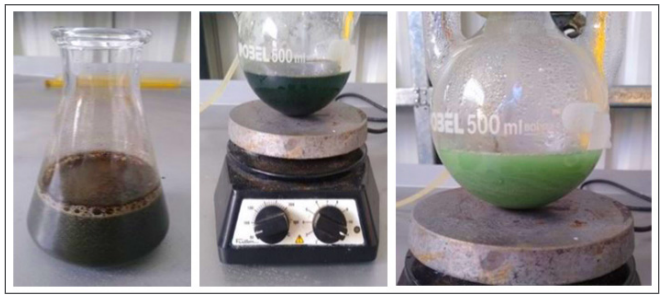
Elements	Concentration
Cobalt	6.5%
Níckel	50%

Source: AAS Laboratory Report (LCA)

3.2. Leaching

For the leaching process, we added 33.33 g of battery powder to 1 L of 2 M sulfuric acid and subjected it to leaching at 89 °C for 4 h with constant stirring (Bertuol et al., 2012). We used a reflux condenser to prevent the loss of leachate volume due to the prolonged duration of this process. Upon initial contact between the powder and the acid, we observed a black effervescent reaction; after 15 minutes, this phenomenon ceased, and the solution turned green, as shown in Figure 6.

Figure 6. Battery leachate



Source: Prepared by the authors

The reaction that takes place during this process is as follows:

$$NiO_{(s)} + H_2SO_{4(aq)} \rightarrow NiSO_{4(aq)} + H_2O_{(l)}$$

$$CoO_{(s)} + H_2SO_{4(aq)} \rightarrow CoSO_{4(aq)} + H_2O_{(l)}$$

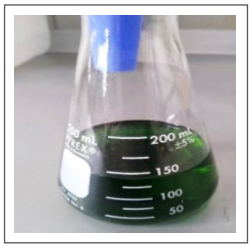
At the end of the leaching process, the suspension was filtered to separate the unleached solid residue from the solution.

Table 4. Unleached mass

	Values	Unit
Total mass	2.792	g
Filter paper mass	1.322	g
Unleached mass	1.470	g

Source: Prepared by the authors

Figure 7. Leachate solution



Source: Prepared by the authors

The pH measured after this process was 1, and this solution was designated as the unpurified electrolyte. Following this process, an atomic absorption analysis was performed to measure the concentration of the various elements present in the unpurified electrolyte, yielding the following results.

Table 5. Concentrations of the main components of the leachate solution

Parameter	Method	Unit	Determination Limit	Leachate 50 - 1
Cobalt	EPA 219.2	mg/l	0.050	1688
Manganese	EPA 243.1	mg/l	0.020	574
Nickel	EPA 249.1	mg/l	0.040	9625
Potassium	EPA 258.1	mg/l	0.210	75
Zinc	EPA 289.2	mg/l	0.038	95

Source: AAS Laboratory Report (LCA)

The results show the presence of several elements in the leachate solution, with a predominance of nickel and cobalt.

We can calculate the leaching % with the following equation:

$$\%X_{Lix} = \frac{C_M * V_{sol}}{m_M} * 100\% \qquad (1)$$

$\%X_{Lix}$: Leaching yield (%)
C_M : Metal concentration (g/L)
V_{sol} : Volume of the leachate solution (L)
m_M : Mass of the leached metal (g)

Table 6. Leaching yield

	Values	Unit
Vol. of leaching solution	1.00	L
Mass in the material	33.33	g
%Co powder	6.50	%
% Ni powder	50.00	%
%Co leached	77.92	%
%Ni leached	57.76	%

Source: Prepared by the authors

The percentage of leached nickel was lower than that of cobalt. This behavior can be attributed to the higher solubility of cobalt sulfates compared to nickel sulfates, and to the adhesion of a fraction of the material to the magnet of the magnetic stirring system. Compared to the use of other acids that yield less than 40% (Zambrano et al., 2018), H_2SO_4 proves to be ideal for this process.

3.3. Removal of rare earths

The removal of rare earths was carried out by selective precipitation. The pH was adjusted to 1.2 by adding 5 M NaOH; the solution was kept under constant stirring for 30 min and subsequently filtered to separate the precipitate.

Table 7. Precipitated mass of rare earths

	Valuees	Unit
Total mass	3.486	g
Filter paper mass	1.251	g
Rare earth mass	2.235	g

Source: Prepared by the authors

3.4. Precipitation of impurities

The solution was adjusted to pH 6 by adding 5 M NaOH to precipitate impurities and keep the nickel and cobalt in solution

Table 8. Precipitated mass of impurities

	Valuees	Unit
Total mass	3.217	g
Filter paper mass	1.405	g
Impurities mass	1.812	g

Source: Prepared by the authors

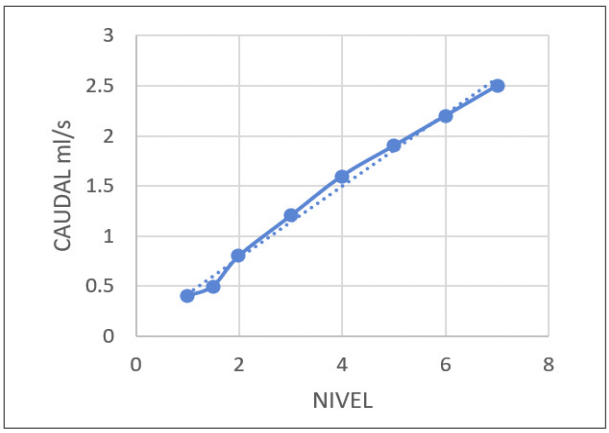
3.5. Electrodeposition

Before establishing the experimental design, preliminary tests were performed to identify the variables with the greatest influence on the electrodeposition.

3.5.1. Flow rate

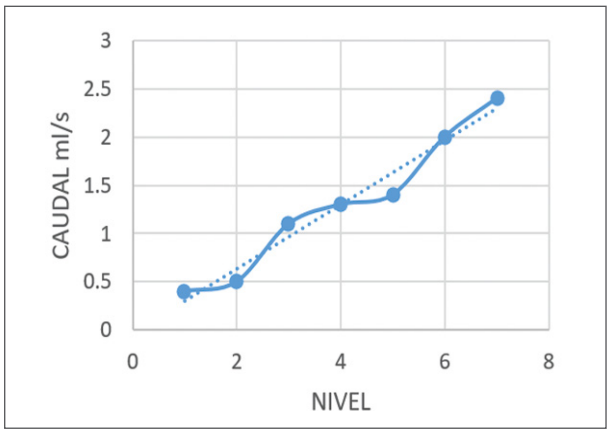
For this variable, the flow rate levels of the peristaltic pumps had to be measured. A time of 10 seconds was used for all measurements.

Figure 8. Level vs. flow rate Pump 1



Source: Prepared by the authors

Figure 9. Level vs. flow rate Pump 2



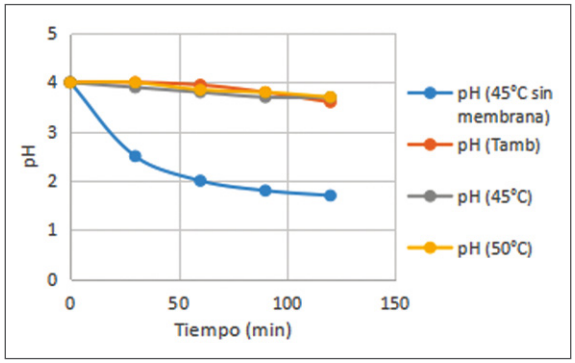
Source: Prepared by the authors

A flow rate of 0.5 mL/s was selected for both pumps, because at this rate, the liquid level in the electrochemical cell remained stable and allowed the maximum possible active area of the electrodes to be utilized.

3.5.2. pH

A pH of 4 was established as a suitable value for the process. To prevent acidification caused by oxidation-reduction reactions, a membrane was used to separate the cathodic and anodic reactions and to reduce sudden variations in pH.

Figure 10. pH variation at different temperatures



Source: Prepared by the authors

3.5.3. Time

Initial tests were performed with an operating time of 1 h; under this condition, no evidence of electrodeposition was observed on the cathode of the electrochemical cell. The first changes were observed at approximately 1 h and 25 min. For this reason, the experimental tests were started at 2 h, a time at which a minimum amount of deposit suitable for measurement and analysis was obtained.

A maximum time of 5 h was established, since at around 5 h and 30 min the deposited solids began to detach, making it difficult to collect the electrodeposit and causing variations in current intensity.

Figure 11. Detachment of the deposit



Source: Prepared by the authors

3.5.4. Temperature

The temperature variable was taken into account for the experimental design, starting from a room temperature of approximately 17 °C up to a maximum value of 45 °C; this second value was chosen because at higher temperatures, solid oxides tend to precipitate in the electrolytic solution.

Figure 12. Electrolyte precipitate



Source: Prepared by the authors

3.5.5. Voltage

$$V_{total} = 6.530\ V$$

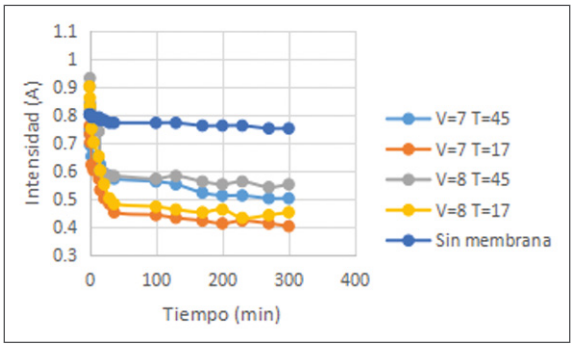
The voltage range was defined based on the electrochemical requirements of the system and preliminary tests.

Preliminary tests were started at 6 V; at this voltage, the formation of the deposit required a prolonged time. Therefore, 7 V was selected as the lower level and 8 V as the upper level. This range was kept within the operating limit of the membrane, whose maximum specified voltage is less than 10 V.

3.5.6. Current intensity

During electrodeposition, the current intensity tended to decrease over time due to the formation of a solid product layer on the cathode surface.

Figure 13. Current intensity vs. time



Source: Prepared by the authors

3.6. Experimental design (Total concentration)

A 2^3 factorial design was applied, supplemented with a center point and an external point. The lower and upper levels of the factors are presented in Table 9.

Table 9. Total concentration design

	Unit	Type	Std. Dev.	Low	High
Temperature	°C	Factor	0	17	45
Time	h	Factor	0	2	5
Voltage	V	Factor	0	7	8
Concentration	%	Response	3.56706	72.82	99.04

Source: Prepared by the authors

The experimental results were analyzed using Design-Expert software, which was used for the statistical analysis of the experimental design and the optimization of the studied variables.

Adesign 2^3 was applied, with 8 experimental tests and a replica (the duplicate of the experiments), obtaining 16 tests, additionally a test was performed for the central point (experiment 17) and another test for the external point (experiment 18), being 18 final experiments shown in Table 10.

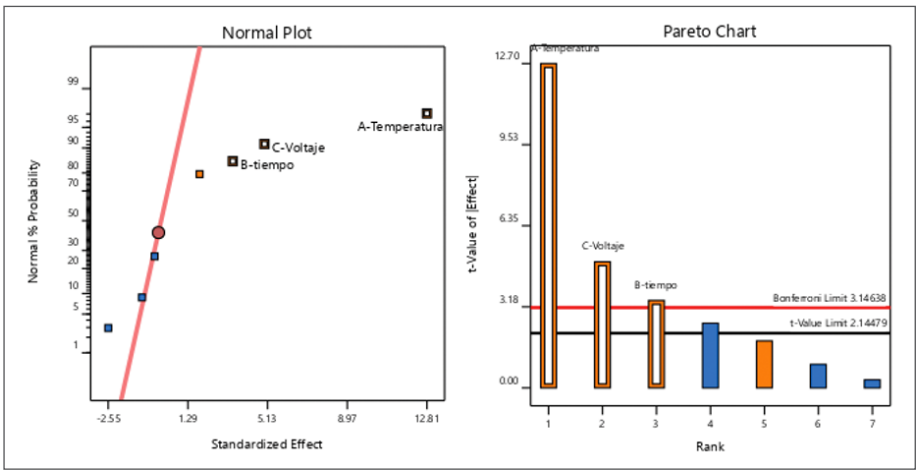
Table 10. Actual Total concentration design

Experiment	Run	Factor 1 A: temperature °C	Factor 2 B: time h	Factor 3 C: voltage V	Response 1 concentration %
1	6	17	2	7	72.82
2	10	17	2	7	75.70
3	13	45	2	7	90.86
4	11	45	2	7	89.70
5	18	17	5	7	83.46
6	5	17	5	7	83.14
7	14	45	5	7	94.28
8	3	45	5	7	93.12
9	1	17	2	8	82.94
10	16	17	2	8	85.49
11	12	45	2	8	95.23
12	17	45	2	8	96.46
13	7	17	5	8	83.89
14	9	17	5	8	83.81
15	8	45	5	8	99.04
16	15	45	5	8	98.21
17	4	30	5	8	91.90
18	2	50	5	8	98.48

Source: Based on the report of the AAS laboratory analysis (IGEMA)

The response variable presented values between 72.82 and 99.04%. The ratio between the maximum and minimum values was 1.36007; since it was less than 3, a data transformation was not considered necessary.

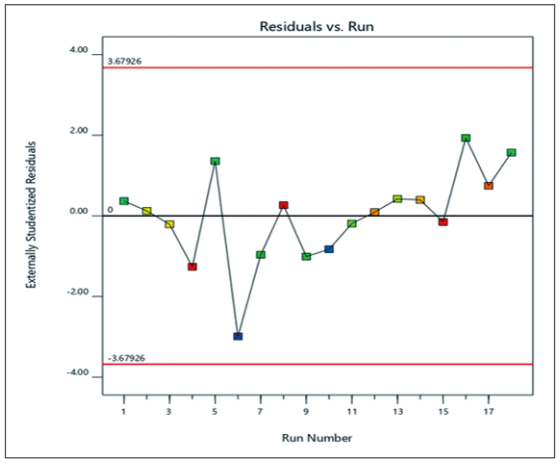
Figure 14. Pareto chart for Total concentration



Source: Design-Expert software

Figure 14 allows for the identification of the variables with the greatest significance in the process.

Figure 15. Residuals for Total concentration



Source: Design-Expert software

The residuals plot shows a data distribution without anomalous observations outside the considered limits.

Table 11. Analysis of variance ANOVA Total concentration

Source	Sum of squares	df	Mean square	F-value	p-value	
Model	969.58	3	323.19	72.13	< 0.0001	significant
A-temperature	722.98	1	722.98	161.36	< 0.0001	
B-time	52.51	1	52.51	11.72	0.0041	
C-voltage	109.21	1	109.21	24.37	0.0002	
Residual	62.73	14	4.48			
Lack of fit	52.83	6	8.80	7.12	0.0071	significant
Pure error	9.90	8	1.24			
Cor Total	1032.31	17				

Source: Design-Expert software

The model F-value of 72.13 implies that the model is significant. There is only a 0.01% chance that an F-value this large could occur due to noise. P-values less than 0.05 indicate statistical significance. In this case, temperature (A), time (B), and voltage (C) were significant factors.

Terms with p-values greater than 0.10 are considered not significant, except for those necessary to maintain model hierarchy.

Table 12. Statistics for Total concentration

Std. Dev.	2.12	R^2	0.9392
Mean	88.81	Adjusted R^2	0.9262
C.V. %	2.38	Predicted R^2	0.8964
		Adeq Precision	23.60

Source: Design-Expert software

The predicted R^2 of 0.8964 is in reasonable agreement with the adjusted R^2 of 0.9262; that is, the difference is less than 0.2. The Adeq Precision parameter evaluates the signal-to-noise ratio; values greater than 4 are considered adequate. The obtained value of 23.60 indicates an adequate signal and supports the use of the model to explore the experimental space.

The coefficient values of the equation corresponding to the concentration of the nickel and cobalt alloy are shown.

$$\%(Ni - Co) = 32.23 + 0.457 * T + 1.153 * t + 4.99 * V$$

3.6.1. Optimization

The values of the variables obtained by maximizing the concentration are:

Table 13. Optimized results Total concentration

Temperature	Time	Voltage	Conc%	Desirability
45.000	5.000	8.000	98.511	0.980
44.998	4.986	8.000	98.494	0.979
45.000	5.000	7.995	98.486	0.979
45.000	4.970	8.000	98.476	0.978
45.000	5.000	7.990	98.461	0.978

Source: Design-Expert software

Therefore, the optimal operating conditions determined were:

Table 14. Optimized values for Total concentration

Temperature	°C	45
Time	h	5
Voltage	V	8
Concentration	%	98.511

Source: Prepared by the authors

4. CONCLUSIONS

- A collection, selection, and pretreatment procedure for end-of-life Ni-MH batteries was established. 30 batteries were processed: 20 AA type, with an average mass of 19.889 g, and 10 AAA type, with an average mass of 11.545 g.

- Manual dismantling allowed the recovery of 148.779 g of anodic material and 171.801 g of cathodic material, equivalent to a total of 320.580 g of active material. For the leaching tests, 33.330 g were used.

- XRF analysis of the battery powder showed that these contain major concentrations of nickel, cobalt, zinc, and potassium, followed to a lesser extent by rare earths and manganese, confirming that they are a viable secondary source of strategic metals.

- AAS analysis shows that the cathodic and anodic powders are composed of 6.5% cobalt and 50% nickel.

- Leaching with 2 M sulfuric acid at 89 °C for 4 h, allowed the metals present in the battery powder to be solubilized, reaching a leaching percentage of 57.76% for nickel and 77.92% for cobalt.

- The applied membrane electrochemical method proved to be viable for the recovery of nickel and cobalt from spent Ni-MH batteries, reaching concentrations higher than 97% (Ni-Co) in the obtained deposits.

- The 2^3 factorial design allowed determining that the optimal combination of conditions to reach total concentrations higher than 97% corresponds to 45 °C, 8 V, and 5 h.

- The F-9010 membrane favored pH control around 4 in the cathodic compartment and contributed to obtaining more uniform deposits with a lower presence of impurities.

5. ACKNOWLEDGMENTS

We thank the Universidad Mayor de San Andrés, in particular the Faculty of Engineering and the Department of Chemical, Petrochemical, Environmental, and Food Engineering, for the facilities provided for the development of this project. Likewise, special recognition is given to the Chemical Processes Research and Development Institute (IIDEPROQ) for its support in the study and development of projects within its different research lines.

6. LIST OF SYMBOLS AND ABBREVIATIONS

Ni - MH: Metallic Nickel Hydride, or Nickel Metal Hydride
F - 9010: Flemion ionic membrane
T: Temperature °C

V: Voltage V
t: Time h
%Ni - Co: Nickel and Cobalt concentration
AAS: Atomic Absorption Spectrophotometry
DRX: X-Ray Diffraction
FRX: X-Ray Fluorescence
kA/m²: Kiloamperes per square meter
M: Molarity mol/Litro
$\%X_{Lix}$: Leaching yield (%)
C_M: Metal concentration (g/L)
V_{sol}: Leached solution volume (L)
m_M: Mass of leached metal (g)

7. REFERENCES

Allied Market Research. (2023). *Nickel-Metal Hydride (Ni-MH) Battery Market Size*, Share Prospects -2027.

Bertuol, D. A., Bernardes, A. M., & Tenório, J.A.S. (2012). Spent NiMH batteries—The role of selective precipitation in the recovery of valuable metals. *Journal of Power Sources*, 193(2), 914-923. https://doi.org/10.1016/j.jpowsour.2009.05.014

Bolrec. (2024). Los residuos tecnológicos también se reciclan. *Bolivia Verifica*.

Hariprakash, B., Shukla, A. K., & Venugoplan, S. (2009a). Secondary batteries – nickel systems | Nickel–Metal Hydride: Overview. En *Encyclopedia of Electrochemical Power Sources* (pp. 494-501). Elsevier. https://doi.org/10.1016/B978-044452745-5.00158-1

Hernandez L., Gonzales M. Alonso A., Legorreta F., (2016). *Recuperación de tierras raras a partir de baterías gastadas tipo Ni-MH*. AMIDIQ. Instituto tecnológico de Celaya departamento de Ingenieria Química ISBN 978-607-95593-4-2

Lu, M., Zhang, H., Wang, B., Zheng, X., & Dai, C. (2013). The Re-Synthesis of LiCoO2 from Spent Lithium-Ion Batteries Separated by Vacuum-Assisted Heat-Treating Method. *International Journal of Electrochemical Science*, 8(6), 8201-8209. https://doi.org/10.1016/S1452-3981(23)12879-3

Lupi C., Pilone D. (2002). Ni–MH spent batteries: a raw material to produce Ni–Co alloys. Waste Management 22 871-874. PII: S0956-053X(02)00074-0Moats, M. S., & Davenport, W. G. (2014). Chapter 2.2—Nickel and Cobalt Production. En S. Seetharaman (Ed.), *Treatise on Process Metallurgy* (pp. 625-669). Elsevier. https://doi.org/10.1016/B978-0-08-096988-6.00026-2

Mordor Intelligence, (2026). *Análisis del tamaño y la participación del mercado del níquel: tendencias de crecimiento y pronóstico* (2026-2031). Mordor Intelligence.

Pagani Martín, C. (2021). *Análisis del proceso químico de recuperación de metales de baterías de vehículos eléctricos* [Info:eu-repo/semantics/bachelorThesis]. E.T.S.I. Diseño Industrial (UPM). https://oa.upm.es/68697/Panasonic. (s. f.). Recuperado 12 de mayo de 2025, de https://www.tempelgroup.com/catalogos/energia/catalogo_baterias_nimh_panasonic.pdf

Rabah M.A., Farghaly F.E. (2008). Recovery of nickel, cobalt and some salts from spent Ni-MH batteries. *Waste Management 28*. https://doi:10.1016/j.wasman.2007.06.007

Rizwan M., Usman K., Alsafran M. (2024). Impactos ecológicos y riesgos potenciales del níquel en los microbios del suelo, las plantas y la salud humana, *Quimosfera Volumen 357*. Elsevier. https://doi.org/10.1016/j.chemosphere.2024.142028

Shin D., Joo., Wang J. Shin M. (2015). *Archivos de Metalurgia y Materiales* https://doi.org/10.1515/amm-2015-0132

Tzanetakis, N., & Scott, K. (2004). Recycling of nickel–metal hydride batteries. II: Electrochemical deposition of cobalt and nickel. *Journal of Chemical Technology & Biotechnology,* 79(9), 927-934. https://doi.org/10.1002/jctb.1082U.S. Geological Survey, Mineral Commodity Summaries (2022). Servicio Geológico de los Estados Unidos https://doi.org/10.3133/mcs2022

Yu, B., Li, Y., Nie, Y., & Mei, H. (2018). High temperature oxidation behavior of a novel cobalt-nickel-base superalloy. *Journal of Alloys and Compounds*, 765, 1148-1157. https://doi.org/10.1016/j.jallcom.2018.06.27

Zambrano-Colmenares, A., Díaz-Salaverría, J., Delvasto, P. (2018). Caracterización de los compuestos químicos obtenidos al emplear ácido acético como agente lixiviante en el tratamiento hidrometalúrgico de pilas Ni-MH desechadas. *Producción + Limpia, 13*(1), 19-29. https://doi.org/10.22507/pml.v13n1a2